



Publication Year	2022
Acceptance in OA @INAF	2023-06-06T14:32:24Z
Title	On the Cosmic Isotropic Background from the radio to the far-ir: a new method for theoretical predictions of the frequency spectrum from monopole to higher multipoles
Authors	BURIGANA, CARLO; TROMBETTI, Tiziana; CHIERICI, FRANCESCO
Handle	http://hdl.handle.net/20.500.12386/34241
Series	ASTRONOMICAL SOCIETY OF THE PACIFIC CONFERENCE SERIES
Number	532

On the Cosmic Isotropic Background from the Radio to the Far-IR: A New Method for Theoretical Predictions of the Frequency Spectrum from Monopole to Higher Multipoles

Carlo Burigana,^{1,2,3} Tiziana Trombetti,¹ and Francesco Chierici^{1,4,5}

¹*INAF, Istituto di Radioastronomia, Via Piero Gobetti 101, I-40129 Bologna, Italy; trombetti@ira.inaf.it*

²*Dipartimento di Fisica e Scienze della Terra, Università di Ferrara, Via Giuseppe Saragat 1, I-44122 Ferrara, Italy*

³*INFN, Sezione di Bologna, Via Irnerio 46, I-40127 Bologna, Italy*

⁴*CNR, Istituto di Scienze Marine, Via Piero Gobetti 101, I-40129 Bologna, Italy*

⁵*INGV, Sezione Roma 2, Via di Vigna Murata 605, I-00143 Roma, Italy*

Abstract. We study how the frequency spectrum of the background isotropic monopole emission is modified and transferred to higher multipoles by boosting effects due to the observer peculiar motion. The method, based on a linear system, is suitable for various background radiation models and here applied to several types of cosmic microwave background (CMB) distorted photon distribution functions and extragalactic background signals superimposed onto the CMB Planckian spectrum, spanning the range between the radio and the far-infrared (far-IR). We derive explicit solutions for the spherical harmonic coefficients up to any desired multipole, ℓ_{\max} , in terms of linear combinations of the signals at just $N = \ell_{\max} + 1$ colatitudes. For appropriate choices of these colatitudes, the symmetry property of the associated Legendre polynomials with respect to $\pi/2$ allows the separation of the system into two subsystems, one for $\ell = 0$ and even multipoles and the other for odd multipoles, and improves the solution accuracy. The simplicity and efficiency of this method can significantly reduce the computational cost needed for accurate predictions on the whole sky and for the scientific analysis of data from future projects. Moreover, in the presence of CMB spectral distortions, this formalism, combined with the representation of CMB intrinsic anisotropies, provides a new test to constrain the intrinsic dipole embedded in the kinematic dipole.

1. Introduction

We study how the frequency spectrum of the background isotropic monopole emission is modified and transferred to higher multipoles by boosting effects due to the observer peculiar motion. The proposed method is suitable for various background radiation models and here applied to several types of cosmic microwave background (CMB) distorted photon distribution functions and extragalactic background signals superimposed onto the CMB Planckian spectrum, from the radio to the far-infrared (far-IR). Its simplicity and efficiency significantly reduces the computational cost needed to per-

form predictions that are accurate enough for applications to scientific analyses of data derived from projects that could be realised even in the very distant future.

2. Framework and formalism

The peculiar velocity effect on the frequency spectrum can be evaluated on the whole sky using the complete description of the Compton-Getting effect (Forman 1970), based on the Lorentz invariance of the photon distribution function, $\eta(\nu)$. In equivalent thermodynamic temperature, $T_{\text{th}}(\nu) = (h\nu/k)/\ln(1 + 1/\eta(\nu))$, the signal observed at the frequency ν is

$$T_{\text{th}}^{\text{BB/dist}}(\nu, \hat{n}, \vec{\beta}) = \frac{xT_0}{\ln(1 + 1/(\eta(\nu, \hat{n}, \vec{\beta}))^{\text{BB/dist}})}, \quad (1)$$

where $\eta(\nu, \hat{n}, \vec{\beta}) = \eta(\nu')$ with $\nu' = \nu(1 - \hat{n} \cdot \vec{\beta}) / (1 - \beta^2)^{1/2}$, \hat{n} is the sky direction unit vector, $\vec{\beta} = \vec{v}/c$ is the observer velocity, $x = h\nu/(kT_r)$ and $T_r = T_0(1 + z)$ are the redshift invariant dimensionless frequency and the redshift dependent effective temperature of the CMB, and ‘BB/dist’ stands for a blackbody spectrum or for any type of non-blackbody signal (Burigana et al. 2018). We expand Eq. (1) in spherical harmonics:

$$T_{\text{th}}^{\text{BB/dist}}(\nu, \theta, \phi, \beta) = \sum_{\ell=0}^{\ell_{\text{max}}} \sum_{m=-\ell}^{\ell} a_{\ell,m}(\nu, \beta) Y_{\ell,m}(\theta, \phi). \quad (2)$$

Adopting a reference system with the z axis parallel to the observer velocity, the dependence on the colatitude θ remains, while that on the longitude ϕ disappears: thus, only the spherical harmonic coefficients $a_{\ell,m}(\nu, \beta)$ with $m = 0$ do not vanish. The amplitude of $a_{\ell,0}(\nu, \beta)$ decreases as $\beta^{\ell \cdot p}$ at increasing multipole, ℓ , with $p \approx 1$ (for a blackbody $p = 1$ and $a_{\ell,0}(\nu, \beta)$ does not depend on ν). Adopting a certain ℓ_{max} in Eq. (2) and computing the signal $T_{\text{th}}^{\text{BB/dist}}$ through Eq. (1) in $N = \ell_{\text{max}} + 1$ sky directions, we can write a system of N linear equations, defined by Eq. (2) with $m = 0$, in the N unknowns $a_{\ell,0}(\nu, \beta)$. Since $\beta \simeq 1.2336 \times 10^{-3}$ (Planck Collaboration 2020), choosing $\ell_{\text{max}} = 6$ allow us to achieve a high numerical accuracy. Furthermore, for appropriate choices of the N colatitudes θ_i , the symmetry property of the associated Legendre polynomials with respect to $\pi/2$ allows the separation of the system into two subsystems, one for $\ell = 0$ and even multipoles and the other for odd multipoles. This improves the system solution accuracy, since the mean error from neglecting higher ℓ 's comes only from $\ell_{\text{max}} + 2$ for even ℓ (or from $\ell_{\text{max}} + 1$ for odd ℓ) (Trombetti et al. 2020). Similar considerations hold for different ℓ_{max} . For $\ell_{\text{max}} = 6$ we select $\theta_i = 0, \pi/4, \pi/3, \pi/2, (2/3)\pi, (3/4)\pi$, and π to simplify the algebra. The two subsystems can be simply solved with the methods of elimination and substitution. For any type of background spectrum, the solution for each $a_{\ell,m}(\nu, \beta)$ is a linear combination of sums and differences of the signals from Eq. (1) at the N colatitudes (Trombetti et al. 2020), namely of:

$$\begin{aligned} & (T_{\text{th}}^{\text{BB/dist}}(\theta = 0) + T_{\text{th}}^{\text{BB/dist}}(\theta = \pi)), \quad (T_{\text{th}}^{\text{BB/dist}}(\theta = \pi/4) + T_{\text{th}}^{\text{BB/dist}}(\theta = (3/4)\pi)), \\ & (T_{\text{th}}^{\text{BB/dist}}(\theta = \pi/3) + T_{\text{th}}^{\text{BB/dist}}(\theta = (2/3)\pi)), \quad \text{and } T_{\text{th}}^{\text{BB/dist}}(\theta = \pi/2) \text{ for } \ell = 0 \text{ and even} \\ & \text{multipoles; and of} \\ & (T_{\text{th}}^{\text{BB/dist}}(\theta = 0) - T_{\text{th}}^{\text{BB/dist}}(\theta = \pi)), \quad (T_{\text{th}}^{\text{BB/dist}}(\theta = \pi/4) - T_{\text{th}}^{\text{BB/dist}}(\theta = (3/4)\pi)), \\ & \text{and } (T_{\text{th}}^{\text{BB/dist}}(\theta = \pi/3) - T_{\text{th}}^{\text{BB/dist}}(\theta = (2/3)\pi)) \text{ for odd multipoles.} \end{aligned}$$

The weights of the signals at the N colatitudes appearing in the solutions show remarkable analogies with the weights for the centred approximation numerical derivative scheme (Fornberg 1988), except the sign alternation because of a mixing of the derivatives entering the problem. This is in principle expected since the solutions at increasing ℓ are tightly related to the derivatives of $\eta(\nu)$ up to the corresponding increasing order, as first pointed out in Danese & De Zotti (1981) for the dipole.

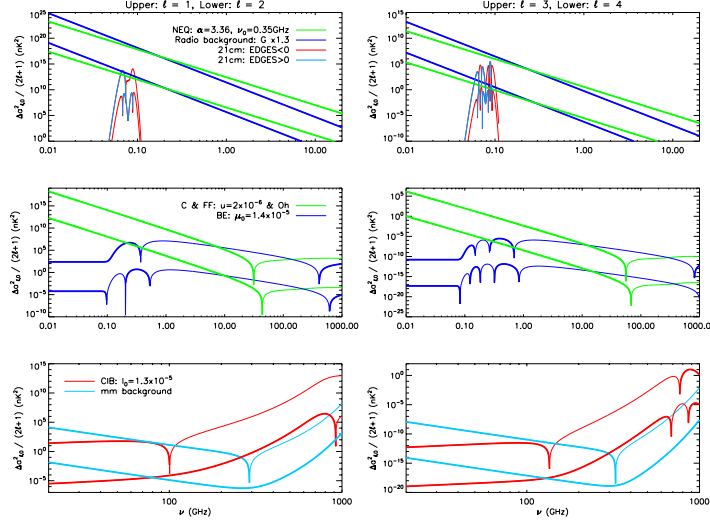


Figure 1. Results for ℓ from 1 to 4 for different models. Thick (or thin) lines correspond to positive (or negative) values of $\Delta a_{\ell,0}(\nu, \beta)$, except for the 21cm redshifted line where the sign of $\Delta a_{\ell,0}(\nu, \beta)$ is given by the colour. *Top (low frequencies)*: CMB non-equilibrium distortion; radio background from extragalactic sources; 21cm redshifted line. *Middle (low and high frequencies)*: CMB Comptonization plus free-free distortion; CMB Bose-Einstein like distortion. *Bottom (high frequencies)*: cosmic infrared background; millimetre background from extragalactic sources.

3. Results

We apply the described method to a blackbody spectrum at temperature $T_0 = 2.72548$ K and a variety of analytical and semi-analytical models for CMB spectral distortions and extragalactic signals, computing the coefficients $a_{\ell,0}(\nu, \beta)$ for ℓ from 0 to $\ell_{\max} = 6$, i.e. for the monopole, dipole, and beyond as in principle measured by a moving observer, assuming for simplicity the almost constant Solar System barycentre velocity. In Fig. 1 we present some results in terms of the square of the difference, $\Delta a_{\ell,0}(\nu, \beta)$, of the $a_{\ell,0}(\nu, \beta)$ for the considered signal and for the blackbody, which is equivalent to the angular power spectrum C_ℓ of the difference of the corresponding maps (see Trombetti et al. (2020) for further details).

Having evaluated the $a_{\ell,0}(\nu, \beta)$ coefficients, it is direct to simulate the all-sky map using Eq. (2) in any reference system. In Fig. 2 we show, in Mollweide projection, the maps for three models minus the map from the blackbody in the reference system with the z axis parallel to the observer velocity (for $\ell = 3$, left) and in Galactic coordinates (for $\ell = 3$, middle, and for $\ell = 6$, right). In each case, the map is displayed at a

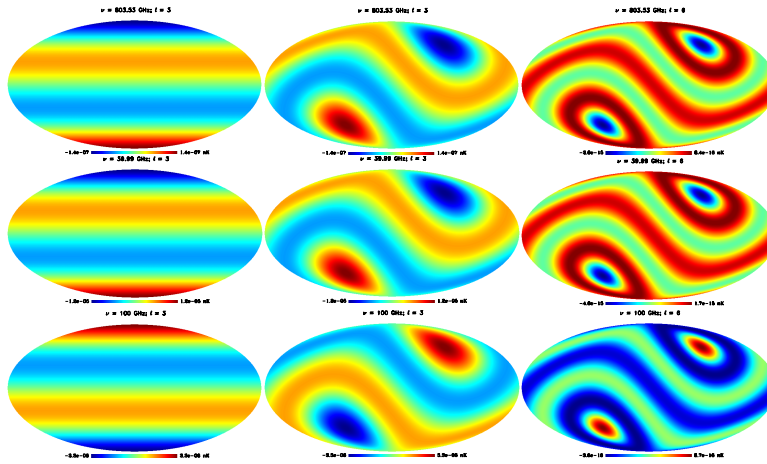


Figure 2. *Top*: CMB Bose-Einstein like distortion. *Middle*: CMB Comptonization alone. *Bottom*: cosmic infrared background. Given its efficiency, the method can easily include the observer motion around the Sun, as combination of maps, each one with almost constant observer velocity: a modulation with an amplitude of $\simeq 8\%$ of the signal and related to the observational strategy is then superimposed onto the longitudinally invariant pattern visible on the left. See Trombetti et al. (2020) for further details. The use of HEALPix (Górski et al. 2005) is acknowledged.

frequency where the imprint of the model is weak, to show the accuracy of the method even for very tiny signals.

4. Constraining the CMB intrinsic dipole

Remarkably, in the presence of spectral distortions, the $a_{\ell,m}(\nu, \beta)$ due to the observer motion have specific frequency dependencies that, while for a generic choice of the reference system are polluted to different m 's, for the z axis parallel to $\vec{\beta}$ obviously appear only at $m = 0$. Intrinsic temperature anisotropies have frequency independent spherical harmonic coefficients, while intrinsic distortion parameters anisotropies depend on ν in a way physically coupled to that of the $a_{\ell,m}(\nu, \beta)$. Thus, in the presence of spectral distortions, except for a degeneracy between the intrinsic temperature anisotropies and peculiar motion induced anisotropies at $\ell = 1$ and $m = 0$, the above different behaviours can be analysed in future CMB surveys to constrain, from the other two m modes, the power, C_1 , of the intrinsic dipole embedded in the kinematic dipole (Trombetti et al. 2020), with implications for inflationary models, universe geometry, and topology.

References

- Burigana, C., Carvalho, C. S., Trombetti, T., et al. 2018, JCAP, 4, 021
 Danese, L., & De Zotti, G. 1981, A&A, 94, L33
 Forman, M. A. 1970, Planet. Space Sci., 18, 25
 Fornberg, B. 1988, Mathematics of Computation, 51, 699
 Górski, K. M., et al. 2005, ApJ, 622, 759
 Planck Collaboration 2020, A&A, 641, A1
 Trombetti, T., Burigana, C., & Chierici, F. 2020, A&A, in press, arXiv:2007.02292